Commun. Comput. Phys.
doi: 10.4208/cicp.091209.080410s

Vol. **9**, No. 3, pp. 520-541
March 2011

Numerical Simulation of Time-Harmonic Waves in Inhomogeneous Media using Compact High Order Schemes

Steven Britt[1], Semyon Tsynkov[1,*] and Eli Turkel[2]

[1] *Department of Mathematics, North Carolina State University, Box 8205, Raleigh, NC 27695, USA.*
[2] *School of Mathematical Sciences, Tel Aviv University, Ramat Aviv, Tel Aviv 69978, Israel.*

Received 9 December 2009; Accepted (in revised version) 8 April 2010

Available online 17 September 2010

Dedicated to the memory of our dear friend, David Gottlieb

Abstract. In many problems, one wishes to solve the Helmholtz equation with variable coefficients within the Laplacian-like term and use a high order accurate method (e.g., fourth order accurate) to alleviate the points-per-wavelength constraint by reducing the dispersion errors. The variation of coefficients in the equation may be due to an inhomogeneous medium and/or non-Cartesian coordinates. This renders existing fourth order finite difference methods inapplicable. We develop a new compact scheme that is provably fourth order accurate even for these problems. We present numerical results that corroborate the fourth order convergence rate for several model problems.

AMS subject classifications: 65N06, 78A48, 78M20

Key words: Helmholtz equation, variable coefficients, high order accuracy, compact finite differences.

1 Introduction

In many problems in computational electrodynamics one considers media with variable properties. Our goal is to obtain high order schemes for the corresponding wave propagation problems. Consider the two dimensional (TE_z) Maxwell equations in frequency

*Corresponding author. *Email addresses:* dsbritt@ncsu.edu (S. Britt), tsynkov@math.ncsu.edu (S. Tsynkov), turkel@post.tau.ac.il (E. Turkel)

space:

$$-i\omega\mu H_z = \frac{\partial E_x}{\partial y} - \frac{\partial E_y}{\partial x},$$
$$-i\omega E_x = \frac{1}{\varepsilon}\frac{\partial H_z}{\partial y}, \qquad i\omega E_y = \frac{1}{\varepsilon}\frac{\partial H_z}{\partial x}.$$

Combining those into a single second order equation, we have:

$$0 = \frac{\partial}{\partial x}\Big(\frac{1}{\varepsilon}\frac{\partial H_z}{\partial x}\Big) + \frac{\partial}{\partial y}\Big(\frac{1}{\varepsilon}\frac{\partial H_z}{\partial y}\Big) + \mu\omega^2 H_z.$$

More generally, we consider the following 2D variable coefficient Helmholtz equation:

$$\frac{\partial}{\partial x}\Big(a(x,y)\frac{\partial u}{\partial x}\Big) + \frac{\partial}{\partial y}\Big(b(x,y)\frac{\partial u}{\partial y}\Big) + k^2(x,y)u(x,y) = 0. \tag{1.1}$$

We emphasize that in many cases it is both easier and cheaper to solve a single second order equation, such as Eq. (1.1), rather than the underlying system of first order equations, see, e.g., [16, 17, 20]. We also stress that the coefficients of Eq. (1.1) vary inside the derivatives. Hence, a straightforward Padé approximation will not work. Because of the pollution effect [3, 6], second order accurate schemes are very inefficient, especially for high frequencies. Our aim is to construct a fourth order accurate finite difference scheme, which would have a compact 9 point stencil in two dimensions (and 27 points in three dimensions). Note that having a small stencil or, in other words, having the same (second) order of the difference equation as that of the differential equation, yet with high order accurate approximation, is convenient, as it considerably simplifies setting the boundary conditions [5, 7] and also leads to a narrower bandwidth of the resulting matrix.

Nehrbass, Jevtic, and Lee studied ways of reducing the phase error [19]. They used a 5 point stencil and replaced the weight of the center node using a Bessel function. Harari and Turkel [15] constructed a fourth order approximation for the Helmholtz equation subject to Dirichlet boundary conditions. The method was based on Padé expansions. It was extended by Singer and Turkel [22] to Neumann boundary conditions. They also introduced an approach referred to as equation based. In this approach, one finds the truncation error of a classical second order method and then uses the Helmholtz equation and its derivatives to eliminate this truncation error to the next order. In both cases, the coefficients a and b in (1.1) were required to be constant, though k could be a smooth function of x and y. A different approach was used by Caruthers, Steinhoff, and Engels [8], who based a difference approximation on Bessel functions. This approach requires that all the coefficients be constant. Under this assumption one can even construct sixth order accurate approximations, see, e.g., [18, 23, 26].

Besides the variation of physical properties of the medium leading to Eq. (1.1), the coefficients of a differential equation may vary because the equation is expressed in non-Cartesian coordinates. In the recent paper [7], we have constructed a fourth order accurate compact finite difference scheme for the Helmholtz equation in polar coordinates. In

that paper, the variation of coefficients was present only in one out of the two coordinate directions (radial). This, in particular, enabled the application of an FFT-based solver and the construction of exact nonlocal artificial boundary conditions for the simulation of waves that scatter off a target and then propagate toward infinity. In this paper our key goal is to allow for the variation of the coefficients a and b in both coordinate directions, and we solve the Helmholtz equation on a bounded domain. For higher wavenumbers, we consider a complex Robin boundary condition to avoid resonances. To construct a compact fourth order accurate scheme, we employ an equation based approach. We note that the paper [7] contains a more detailed bibliography survey.

For the most part, the analysis in the current paper addresses the two-dimensional case. However, in Section 3 we show that the extension to three dimensions is straightforward.

2 2D variable coefficient Helmholtz equation

We now construct a compact fourth order accurate finite difference scheme for the variable coefficient Helmholtz equation (1.1).

First, we reformulate Eq. (1.1) as formal ODEs given by

$$\frac{\partial}{\partial x}\Big(a(x,y)\frac{\partial u}{\partial x}\Big)=F_x\overset{\text{def}}{=}f-k^2u-\frac{\partial}{\partial y}\Big(b(x,y)\frac{\partial u}{\partial y}\Big), \tag{2.1a}$$

and

$$\frac{\partial}{\partial y}\Big(b(x,y)\frac{\partial u}{\partial y}\Big)=F_y\overset{\text{def}}{=}f-k^2u-\frac{\partial}{\partial x}\Big(a(x,y)\frac{\partial u}{\partial x}\Big). \tag{2.1b}$$

Then, we approximate the left-hand sides of (2.1a) and (2.1b) at the grid node (m,n) with second order accuracy as follows:

$$\frac{\partial}{\partial x}\Big(a(x,y)\frac{\partial u}{\partial x}\Big)=\frac{1}{h}\Big(a_{m+\frac{1}{2},n}\frac{u_{m+1,n}-u_{m,n}}{h}-a_{m-\frac{1}{2},n}\frac{u_{m,n}-u_{m-1,n}}{h}\Big)+\mathcal{O}(h^2), \tag{2.2a}$$

and

$$\frac{\partial}{\partial y}\Big(b(x,y)\frac{\partial u}{\partial y}\Big)=\frac{1}{h}\Big(b_{m,n+\frac{1}{2}}\frac{u_{m,n+1}-u_{m,n}}{h}-b_{m,n-\frac{1}{2}}\frac{u_{m,n}-u_{m,n-1}}{h}\Big)+\mathcal{O}(h^2). \tag{2.2b}$$

Adding (2.2a) and (2.2b) and then approximating the non-differentiated term and the right-hand side of (1.1) as $\big(k^2u\big)_{m,n}$ and $f_{m,n}$ respectively, we obtain a second order approximation of (1.1). Our aim is to extend (2.2) to a fourth order accurate approximation.

Analysis of the truncation error for the finite differences of (2.2) yields the following:

$$\begin{aligned}&\frac{1}{h}\Big(a_{m+\frac{1}{2},n}\frac{u_{m+1,n}-u_{m,n}}{h}-a_{m-\frac{1}{2},n}\frac{u_{m,n}-u_{m-1,n}}{h}\Big)\\&=\frac{\partial}{\partial x}\Big(a(x,y)\frac{\partial u}{\partial x}\Big)+\frac{h^2}{12}\Big(au_{xxxx}+2a_xu_{xxx}+\frac{3a_{xx}u_{xx}}{2}+\frac{a_{xxx}u_x}{2}\Big)+\mathcal{O}(h^4),\end{aligned}\tag{2.3a}$$

$$\begin{aligned}&\frac{1}{h}\Big(b_{m,n+\frac{1}{2}}\frac{u_{m,n+1}-u_{m,n}}{h}-b_{m,n-\frac{1}{2}}\frac{u_{m,n}-u_{m,n-1}}{h}\Big)\\&=\frac{\partial}{\partial y}\Big(b(x,y)\frac{\partial u}{\partial y}\Big)+\frac{h^2}{12}\Big(bu_{yyyy}+2b_yu_{yyy}+\frac{3b_{yy}u_{yy}}{2}+\frac{b_{yyy}u_y}{2}\Big)+\mathcal{O}(h^4).\end{aligned}\tag{2.3b}$$

In order to eliminate the $\mathcal{O}(h^2)$ error terms in (2.3a), we first differentiate the ODE (2.1a) twice in x and obtain a system of three equations with respect to u_{xx}, u_{xxx}, and u_{xxxx}:

$$a_xu_x+au_{xx}=F_x,\tag{2.4a}$$

$$a_{xx}u_x+2a_xu_{xx}+au_{xxx}=\frac{\partial F_x}{\partial x},\tag{2.4b}$$

$$a_{xxx}u_x+3a_{xx}u_{xx}+3a_xu_{xxx}+au_{xxxx}=\frac{\partial^2F_x}{\partial x^2}.\tag{2.4c}$$

Solving each equation of (2.4) for the highest derivative of u, we obtain

$$u_{xx}=\frac{1}{a}(F_x-a_xu_x),\tag{2.5a}$$

$$u_{xxx}=\frac{1}{a}\Big(\frac{\partial F_x}{\partial x}-a_{xx}u_x-2a_xu_{xx}\Big),\tag{2.5b}$$

$$u_{xxxx}=\frac{1}{a}\Big(\frac{\partial^2F_x}{\partial x^2}-a_{xxx}u_x-3a_{xx}u_{xx}-3a_xu_{xxx}\Big).\tag{2.5c}$$

Substituting (2.5a) into (2.5b) and substituting (2.5a) and (2.5b) into (2.5c), we arrive at equations that contain only first derivatives of u on the right-hand side:

$$u_{xx}=\frac{1}{a}(F_x-a_xu_x),\tag{2.6a}$$

$$u_{xxx}=\frac{1}{a}\Big(\frac{\partial F_x}{\partial x}-a_{xx}u_x-\frac{2a_x}{a}(F_x-a_xu_x)\Big),\tag{2.6b}$$

$$u_{xxxx}=\frac{1}{a}\Big[\frac{\partial^2F_x}{\partial x^2}-a_{xxx}u_x-\frac{3a_{xx}}{a}(F_x-a_xu_x)-\frac{3a_x}{a^2}\Big(\frac{\partial F_x}{\partial x}-a_{xx}u_x-\frac{2a_x}{a}(F_x-a_xu_x)\Big)\Big].\tag{2.6c}$$

By substituting expressions (2.6a), (2.6b), and (2.6c) for u_{xx}, u_{xxx}, and u_{xxxx}, respectively, into the $\mathcal{O}(h^2)$ terms on the right-hand side of (2.3a), we get

$$\begin{aligned}&au_{xxxx}+2a_xu_{xxx}+\frac{3a_{xx}u_{xx}}{2}+\frac{a_{xxx}u_x}{2}\\&=\frac{\partial^2F_x}{\partial x^2}-\frac{a_x}{a}\frac{\partial F_x}{\partial x}+\Big(\frac{2a_x^2}{a^2}-\frac{3a_{xx}}{2a}\Big)F_x+\Big(-\frac{a_{xxx}}{2}+\frac{5a_{xx}a_x}{2a}-\frac{2a_x^3}{a^2}\Big)u_x.\end{aligned}\tag{2.7}$$

In order to achieve an overall fourth order accuracy for (2.3a), it is sufficient to approximate the terms multiplied by $h^2/12$ with second order accuracy. So we need to approximate the right-hand side of (2.7) with second order accuracy. For simplicity, assume that all derivatives of a and b on the right-hand side of (2.7) are known analytically.[†] Then, we find expressions for F_x, $\partial F_x/\partial x$, and $\partial^2 F_x/\partial x^2$, which is done with the help of formula (2.1a):

$$F_x = f - k^2 u - b_y u_y - b u_{yy}, \tag{2.8a}$$

$$\frac{\partial F_x}{\partial x} = f_x - \left[b_{xy}u_y + b_y u_{xy} + b_x u_{yy} + b u_{yyx} + (k^2 u)_x\right], \tag{2.8b}$$

$$\frac{\partial^2 F_x}{\partial x^2} = f_{xx} - \left[b_{yxx}u_y + 2b_{yx}u_{yx} + b_y u_{yxx} + b_{xx}u_{yy} + 2b_x u_{yyx} + b u_{yyxx} + (k^2 u)_{xx}\right]. \tag{2.8c}$$

We use the standard five node stencil to approximate $(k^2u)_x$, $(k^2u)_{xx}$, u_y, u_{yy}, f_x, and f_{xx} in (2.8) by central differences with second order accuracy. We then approximate the remaining terms u_{xy}, u_{yyx}, u_{xxy}, and u_{xxyy} on a compact 3×3 stencil (which contains four additional corner nodes) also with second order accuracy as follows:

$$\begin{aligned}
u_{xy} &= \frac{1}{2h}\Big(\frac{u_{m+1,n+1}-u_{m-1,n+1}}{2h} - \frac{u_{m+1,n-1}-u_{m-1,n-1}}{2h}\Big) + \mathcal{O}(h^2),\\
u_{xxy} &= \frac{1}{h^2}\Big(\frac{u_{m+1,n+1}-u_{m+1,n-1}}{2h} + \frac{u_{m-1,n+1}-u_{m-1,n-1}}{2h} - 2\frac{u_{m,n+1}-u_{m,n-1}}{2h}\Big) + \mathcal{O}(h^2),\\
u_{yyx} &= \frac{1}{h^2}\Big(\frac{u_{m+1,n+1}-u_{m-1,n+1}}{2h} + \frac{u_{m+1,n-1}-u_{m-1,n-1}}{2h} - 2\frac{u_{m+1,n}-u_{m-1,n}}{2h}\Big) + \mathcal{O}(h^2),\\
u_{xxyy} &= \frac{1}{h^2}\Big(\frac{u_{m+1,n+1}+u_{m+1,n-1}-2u_{m+1,n}}{h^2} + \frac{u_{m-1,n+1}+u_{m-1,n-1}-2u_{m-1,n}}{h^2}\\
&\qquad -2\frac{u_{m,n+1}+u_{m,n-1}+2u_{m,n}}{h^2})\Big) + \mathcal{O}(h^2).
\end{aligned}$$

Altogether, we obtain a second order accurate approximation of all the terms on the right-hand sides of equalities (2.8) on a 3×3 stencil:

$$F_x = f_{m,n} - (k^2u)_{m,n} - \frac{b_y}{2h}(u_{m,n+1}-u_{m,n-1}) - b\frac{u_{m,n+1}-2u_{m,n}+u_{m,n-1}}{h^2} + \mathcal{O}(h^2), \tag{2.9a}$$

$$\begin{aligned}
\frac{\partial F_x}{\partial x} &= f_x - \left[b_{xy}u_y + b_y u_{xy} + b_x u_{yy} + b u_{yyx} + (k^2u)_x\right]\\
&= \frac{f_{m+1,n}-f_{m-1,n}}{2h} - \Big[\frac{b_{xy}}{2h}(u_{m,n+1}-u_{m,n-1}) + \frac{b_y}{4h^2}(u_{m+1,n+1}-u_{m-1,n+1}\\
&\quad -u_{m+1,n-1}+u_{m-1,n-1}) + \frac{b_x}{h^2}(u_{m,n+1}+u_{m,n-1}-2u_{m,n}) + \frac{b}{2h^3}(u_{m+1,n+1}-u_{m-1,n+1}\\
&\quad +u_{m+1,n-1}-u_{m-1,n-1}-2(u_{m+1,n}-u_{m-1,n})) + \frac{(k^2u)_{m+1,n}-(k^2u)_{m-1,n}}{2h}\Big] + \mathcal{O}(h^2),
\end{aligned} \tag{2.9b}$$

[†]Otherwise, we can also replace them by finite differences, although this may require a larger stencil.

$$\begin{aligned}\frac{\partial^2 F_x}{\partial x^2} &= f_{xx}-[b_{yxx}u_y+2b_{yx}u_{yx}+b_y u_{yxx}+b_{xx}u_{yy}+2b_x u_{yyx}+bu_{yyxx}+(k^2u)_{xx}]\\ &= \frac{f_{m+1,n}+f_{m-1,n}-2f_{m,n}}{h^2}-\Big[\frac{b_{yxx}}{2h}(u_{m,n+1}-u_{m,n-1})+\frac{b_{yx}}{2h^2}(u_{m+1,n+1}-u_{m-1,n+1}\\ &\quad -u_{m+1,n-1}+u_{m-1,n-1})+\frac{b_y}{2h^3}(u_{m+1,n+1}-u_{m+1,n-1}+u_{m-1,n+1}-u_{m-1,n-1}\\ &\quad -2(u_{m,n+1}-u_{m,n-1}))+\frac{b_{xx}}{h^2}(u_{m,n+1}+u_{m,n-1}-2u_{m,n})+\frac{b_x}{h^3}(u_{m+1,n+1}-u_{m-1,n+1}\\ &\quad +u_{m+1,n-1}-u_{m-1,n-1}-2(u_{m+1,n}-u_{m-1,n}))+\frac{b}{h^4}(u_{m+1,n+1}+u_{m+1,n-1}\\ &\quad +u_{m-1,n+1}+u_{m-1,n-1}+4u_{m,n}-2(u_{m,n+1}+u_{m,n-1}+u_{m+1,n}+u_{m-1,n}))\\ &\quad +\frac{(k^2u)_{m+1,n}-2(k^2u)_{m,n}+(k^2u)_{m-1,n}}{h^2}\Big]. \end{aligned} \tag{2.9c}$$

Since there is symmetry between the derivatives in the x and y directions, the entire previous argument can be duplicated in the y direction. Namely, we start with differentiating equation (2.1b) twice in y [cf. formula (2.4)], and then we express the $\mathcal{O}(h^2)$ term on the right hand side of (2.3b) via u_y, F_y, $\partial F_y/\partial y$, and $\partial^2 F_y/\partial y^2$ [cf. formula (2.7)]. In order to obtain a compact discretization, we approximate the resulting terms with second order accuracy on a 3×3 stencil, yielding:

$$F_y = f_{m,n}-(k^2)u_{m,n}-\frac{a_x}{2h}(u_{m+1,n}-u_{m-1,n})-a\frac{u_{m+1,n}-2u_{m,n}+u_{m-1,n}}{h^2}+\mathcal{O}(h^2), \tag{2.10a}$$

$$\begin{aligned}\frac{\partial F_y}{\partial y} &= f_y-[a_{xy}u_x+a_x u_{xy}+a_y u_{xx}+au_{xxy}+(k^2u)_y]\\ &= \frac{f_{m,n+1}-f_{m,n-1}}{2h}-\Big[\frac{a_{xy}}{2h}(u_{m+1,n}-u_{m-1,n})+\frac{a_x}{4h^2}(u_{m+1,n+1}-u_{m-1,n+1}\\ &\quad -u_{m+1,n-1}+u_{m-1,n-1})+\frac{a_y}{h^2}(u_{m+1,n}+u_{m-1,n}-2u_{m,n})+\frac{a}{2h^3}(u_{m+1,n+1}\\ &\quad -u_{m+1,n-1}+u_{m-1,n+1}-u_{m-1,n-1}-2(u_{m,n+1}-u_{m,n-1}))\\ &\quad +\frac{(k^2u)_{m,n+1}-(k^2u)_{m,n-1}}{2h}\Big]+\mathcal{O}(h^2), \end{aligned} \tag{2.10b}$$

$$\begin{aligned}\frac{\partial^2 F_y}{\partial y^2} &= f_{yy}-[a_{xyy}u_x+2a_{xy}u_{xy}+a_x u_{xyy}+a_{yy}u_{xx}+2a_y u_{xxy}+au_{xxyy}+(k^2u)_{yy}]\\ &= \frac{f_{m,n+1}+f_{m,n-1}-2f_{m,n}}{h^2}-\Big[\frac{a_{xyy}}{2h}(u_{m+1,n}-u_{m-1,n})+\frac{a_{xy}}{2h^2}(u_{m+1,n+1}-u_{m-1,n+1}\\ &\quad -u_{m+1,n-1}+u_{m-1,n-1})+\frac{a_x}{2h^3}(u_{m+1,n+1}-u_{m-1,n+1}+u_{m+1,n-1}-u_{m-1,n-1}\\ &\quad -2(u_{m+1,n}-u_{m-1,n}))+\frac{a_{yy}}{h^2}(u_{m+1,n}+u_{m-1,n}-2u_{m,n})+\frac{a_y}{h^3}(u_{m+1,n+1}\\ &\quad -u_{m+1,n-1}+u_{m-1,n+1}-u_{m-1,n-1}-2(u_{m,n+1}-u_{m,n-1}))+\frac{b}{h^4}(u_{m+1,n+1}\\ &\quad +u_{m+1,n-1}+u_{m-1,n+1}+u_{m-1,n-1}+4u_{m,n}-2(u_{m,n+1}+u_{m,n-1}+u_{m+1,n}\\ &\quad +u_{m-1,n}))+\frac{(k^2u)_{m,n+1}-2(k^2u)_{m,n}+(k^2u)_{m,n-1}}{h^2}\Big]. \end{aligned} \tag{2.10c}$$

Finally, assembling all the terms, we obtain a fourth order accurate approximation for Eq. (1.1) on a compact 3×3 stencil:

$$\begin{aligned}
&\frac{1}{h}\Big(a_{m+\frac{1}{2},n}\frac{u_{m+1,n}-u_{m,n}}{h}-a_{m-\frac{1}{2},n}\frac{u_{m,n}-u_{m-1,n}}{h}\Big)+\frac{1}{h}\Big(b_{m,n+\frac{1}{2}}\frac{u_{m,n+1}-u_{m,n}}{h}\\
&\quad -b_{m,n-\frac{1}{2}}\frac{u_{m,n}-u_{m,n-1}}{h}\Big)-\frac{h^2}{12}\Big[\frac{\partial^2 F_x}{\partial x^2}-\frac{a_x}{a}\frac{\partial F_x}{\partial x}+\Big(\frac{2a_x^2}{a^2}-\frac{3a_{xx}}{2a}\Big)F_x+\Big(-\frac{a_{xxx}}{2}\\
&\quad +\frac{5a_{xx}a_x}{2a}-\frac{2a_x^3}{a^2}\Big)\frac{u_{m+1,n}-u_{m-1,n}}{2h}\Big]\Big|_{m,n}-\frac{h^2}{12}\Big[\frac{\partial^2 F_y}{\partial y^2}-\frac{b_y}{b}\frac{\partial F_y}{\partial y}+\Big(\frac{2b_y^2}{b^2}-\frac{3b_{yy}}{2b}\Big)F_y\\
&\quad +\Big(-\frac{b_{yyy}}{2}+\frac{5b_{yy}b_y}{2b}-\frac{2b_y^3}{b^2}\Big)\frac{u_{m,n+1}-u_{m,n-1}}{2h}\Big]\Big|_{m,n}+(k^2u)_{m,n}=f_{m,n}. \qquad (2.11)
\end{aligned}$$

In formula (2.11), the terms in parentheses premultiplied by $h^2/12$ are evaluated on the grid with second order accuracy using formulae (2.9) and (2.10).

3 Three dimensions

The extension to three dimensions is straightforward. The Helmholtz equation (1.1) is replaced by

$$\frac{\partial}{\partial x}\Big(a(x,y,z)\frac{\partial u}{\partial x}\Big)+\frac{\partial}{\partial y}\Big(b(x,y,z)\frac{\partial u}{\partial y}\Big)+\frac{\partial}{\partial z}\Big(c(x,y,z)\frac{\partial u}{\partial z}\Big)+k^2(x,y,z)u=0. \qquad (3.1)$$

Then, Eq. (2.1a) is replaced by

$$\frac{\partial}{\partial x}\Big(a\frac{\partial u}{\partial x}\Big)=F_x\overset{\text{def}}{=}f-k^2u-\frac{\partial}{\partial y}\Big(b\frac{\partial u}{\partial y}\Big)-\frac{\partial}{\partial z}\Big(c\frac{\partial u}{\partial z}\Big), \qquad (3.2)$$

and similarly for the other two coordinates. The derivation from formula (2.2) through formula (2.7) remains as before. Finally, Eq. (2.8) are replaced by

$$\begin{aligned}
&F_x=f-k^2u-\frac{\partial}{\partial y}\Big(b\frac{\partial u}{\partial y}\Big)-\frac{\partial}{\partial z}\Big(c\frac{\partial u}{\partial z}\Big),\\
&\frac{\partial F_x}{\partial x}=f_x-(k^2u)_x-\frac{\partial^2}{\partial x\partial y}\Big(b\frac{\partial u}{\partial y}\Big)-\frac{\partial^2}{\partial x\partial z}\Big(c\frac{\partial u}{\partial z}\Big),\\
&\frac{\partial^2 F_x}{\partial x^2}=f_{xx}-(k^2u)_{xx}-\frac{\partial^3}{\partial^2 x\partial y}\Big(b\frac{\partial u}{\partial y}\Big)-\frac{\partial^3}{\partial^2 x\partial z}\Big(c\frac{\partial u}{\partial z}\Big).
\end{aligned}$$

Replacing the derivatives by finite differences as in (2.9) and similarly in the y and z directions results in a compact $3\times 3\times 3$ stencil.

4 Boundary conditions

In order to maintain high order accuracy, it is necessary that all the boundary conditions be accurate to the same order as the interior scheme, see [11].

4.1 Dirichlet boundary condition

We first consider the variable coefficient Helmholtz equation with constant wavenumber k on a square domain $D=\{(x,y)|-s/2<x<s/2,\ -s/2<y<s/2\}$:

$$-\frac{\partial}{\partial x}\Big(a\frac{\partial u}{\partial x}\Big)-\frac{\partial}{\partial y}\Big(b\frac{\partial u}{\partial y}\Big)-k^2u=-f,\qquad (x,y)\in D, \tag{4.1}$$

subject to a zero Dirichlet boundary condition:

$$u(x,y)=0,\quad \text{when}\ \ x=\pm\frac{s}{2}\quad \text{or}\quad y=\pm\frac{s}{2}. \tag{4.2}$$

The assumption $k=\text{const}$ is not necessary, and is introduced in Eq. (4.1) only for convenience.

Discretization of the Dirichlet boundary condition (4.2) is completely straightforward. Consider a Cartesian grid on the square D:

$$\Big\{(x_m,y_n)\Big|m=-\frac{M}{2},\cdots,\frac{M}{2},\quad n=-\frac{M}{2},\cdots,\frac{M}{2}\Big\}, \tag{4.3}$$

where

$$M=\frac{s}{h},\qquad x_m=m\cdot h,\qquad y_n=n\cdot h.$$

Since the scheme (2.11) is built on a compact 3×3 stencil, it does not require any additional "numerical" boundary conditions, and we simply approximate (4.2) as follows

$$u_{m,n}=0,\quad \text{if}\ \ m=\pm\frac{M}{2}\quad \text{or}\quad n=\pm\frac{M}{2},$$

which yields fourth order accuracy.

It is known, however, that when solving the Helmholtz equation on a bounded domain subject to a Dirichlet boundary condition, resonances may occur, which means that the solution may become non-unique.[‡] To avoid this undesirable phenomenon, we employ additional considerations when choosing the wavenumber k.

Let the variable coefficients $a=a(x,y)$ and $b=b(x,y)$ in Eq. (4.1) be smooth and bounded on $\bar{D}$. In addition, we require that

$$\nu\overset{\text{def}}{=}\min\Big\{\min_{(x,y)\in\bar{D}}a(x,y),\ \min_{(x,y)\in\bar{D}}b(x,y)\Big\}>0. \tag{4.4}$$

Inequality (4.4) implies, in particular, that the operator

$$Lu\equiv-\frac{\partial}{\partial x}\Big(a\frac{\partial u}{\partial x}\Big)-\frac{\partial}{\partial y}\Big(b\frac{\partial u}{\partial y}\Big), \tag{4.5}$$

[‡]It is common in the diffraction theory to refer to the loss of uniqueness by the solution as to a resonance. This happens when the wavenumber (squared) in the Helmholtz equation appears to be an eigenvalue of the corresponding negative Laplacian.

subject to the same Dirichlet boundary condition (4.2) is self-adjoint and positive definite on the space $W^2_{2,0}(D)$.[§] To guarantee uniqueness of the solution u to problem (4.1) with boundary condition (4.2), we need to ensure that k^2 is not an eigenvalue of the operator L of (4.5), (4.2). This is done by estimating the smallest eigenvalue $\lambda_{\min}$ of L, i.e., its eigenvalue closest to zero, and then choosing k accordingly.

As shown in [25, Section 150], the following estimate holds for the smallest eigenvalue of L:

$$\lambda_{\min} \geq \frac{\nu}{c_D},$$

where ν is defined in formula (4.4), and c_D is the constant from the Friedrichs inequality. For a square domain, it is easy to prove (see [24, Section 115]) that $c_D = s^2$ (the area of the square). Consequently:

$$\lambda_{\min} \geq \frac{\nu}{s^2}. \tag{4.6}$$

Inequality (4.6) implies that choosing the wavenumber k so that

$$k^2 < \frac{\nu}{s^2} \tag{4.7}$$

is sufficient for avoiding the resonances and hence guaranteeing uniqueness of the solution, see [1,2], since then the sum $\lambda_{\min} - k^2$ will remain positive.

In fact, estimate (4.6) is conservative and can be sharpened. If, for example, L is the negative Laplace operator so that $a \equiv b \equiv 1$ and $\nu = 1$, then the first eigenfunction is $v = \cos(\pi x/s)\cos(\pi y/s)$ and the minimum eigenvalue is $\lambda_{\min} = 2\pi^2/s^2$. Hence, for practical purposes we freeze coefficients and estimate the minimum eigenvalue of L by merely replacing the coefficients a and b in (4.5) by their minimum value ν of (4.4). This leads to a weaker constraint on k instead of (4.7):

$$k^2 < \frac{2\pi^2\nu}{s^2}. \tag{4.8}$$

In the numerical experiments of Section 5.1, we make sure that inequality (4.8) holds. We emphasize that this is a sufficient but not necessary condition for the solution to be unique.

4.2 Local Sommerfeld-type boundary conditions

To be able to test the performance of the scheme for larger values of k, the constraint given by inequality (4.8) must be alleviated. A convenient way of doing that is to change the boundary condition so that the problem is no longer self-adjoint. Then, its spectrum becomes essentially complex, and no real value k^2 can be an eigenvalue.

[§]This space is a completion in the norm $W^2_2(D)$ of the set of functions $C^2_0(\bar{D}) \subset C^2(\bar{D})$ that are twice continuously differentiable on $\bar{D}$ and are equal to zero on ∂D. For self-adjointness on $W^2_{2,0}(D)$, in addition to (4.4) one also needs to require an upper bound on the coefficients a and b, and on absolute values of their first derivatives, see [25, Sections 145, 148, 149].

In [11], Erlangga and Turkel derive a fourth order accurate scheme for a simplified absorbing boundary condition

$$\frac{\partial u}{\partial x}+i\beta u=0.$$

Furthermore, they present computational evidence that if the interior scheme is fourth order accurate but the absorbing boundary condition is only second order accurate, then the global accuracy is second order.

Hereafter, we set the local Sommerfeld-type, i.e., complex Robin, boundary conditions on two opposite sides of the square D:

$$\frac{\partial u}{\partial x}+iku=0, \quad \text{if } x=\frac{s}{2}, \tag{4.9a}$$

$$\frac{\partial u}{\partial x}-iku=0, \quad \text{if } x=-\frac{s}{2}, \tag{4.9b}$$

and keep a homogeneous Dirichlet boundary condition on the other pair of opposite sides:

$$u(x,y)=0, \quad \text{if } y=\pm\frac{s}{2}. \tag{4.10}$$

We emphasize that we do not intend to simulate the radiation of waves toward infinity by means of boundary conditions (4.9a) and (4.9b). The problem is still solved on a bounded region (a square), and our goal is rather to avoid the eigenvalues in the interior.

Boundary conditions (4.9a) and (4.9b) are approximated on the grid with fourth order accuracy using compact differencing. For convenience, they are set at half-nodes:¶

$$u_{x_{M-\frac{1}{2},n}}+iku_{M-\frac{1}{2},n}=0, \tag{4.11a}$$

$$u_{x_{\frac{1}{2},n}}-iku_{\frac{1}{2},n}=0. \tag{4.11b}$$

We will treat the left boundary of the square $x=-s/2$, and the analogous case of the right boundary $x=s/2$ will follow by symmetry. First, we approximate (4.11b) with second order accuracy as follows:

$$u_{x_{\frac{1}{2},n}}-iku_{\frac{1}{2},n}=\frac{u_{1,n}-u_{0,n}}{h}-\frac{(h/2)^2}{6}u_{xxx_{\frac{1}{2},n}}-ik\frac{u_{1,n}+u_{0,n}}{2}+ik\frac{(h/2)^2}{2}u_{xx_{\frac{1}{2},n}}+\mathcal{O}(h^4). \tag{4.12}$$

In order to eliminate the $\mathcal{O}(h^2)$ terms in (4.12), it is sufficient to approximate the derivatives $(u_{xxx})_{1/2,n}$ and $(u_{xx})_{1/2,n}$ with second order accuracy. We will use formulae (2.6a) and (2.6b), taking into account that since $f(x,y)$ is compactly supported inside the square,

¶As shown in [11], we can also obtain a fourth order accurate approximation to (4.9) with the boundary condition imposed at a full node.

we can assume that near the boundary $f\equiv 0$. For the derivative $(u_{xx})_{1/2,n}$, this yields:

$$\begin{aligned}u_{xx_{\frac{1}{2},n}}=&\frac{1}{a}(F_x-a_xu_x)\Big|_{\frac{1}{2},n}\\=&\frac{1}{a_{\frac{1}{2},n}}\Big(-(k^2u)_{\frac{1}{2},n}-b_{y_{\frac{1}{2},n}}\frac{u_{\frac{1}{2},n+1}-u_{\frac{1}{2},n-1}}{h}\\&-b_{\frac{1}{2},n}\frac{u_{\frac{1}{2},n+1}-2u_{\frac{1}{2},n}+u_{\frac{1}{2},n-1}}{(h/2)^2}-a_{x_{\frac{1}{2},n}}\frac{u_{1,n}-u_{0,n}}{h}\Big)+\mathcal{O}(h^2).\end{aligned}\tag{4.13}$$

Similarly, for $(u_{xxx})_{1/2,n}$ we obtain:

$$\begin{aligned}u_{xxx_{\frac{1}{2},n}}=&\frac{1}{a}\Big(\frac{\partial F_x}{\partial x}-a_{xx}u_x-\frac{2a_x}{a}(F_x-a_xu_x)\Big)\Big|_{\frac{1}{2},n}\\=&\frac{1}{a_{\frac{1}{2},n}}\Big[-\Big(\frac{b_{xy_{\frac{1}{2},n}}}{h}(u_{\frac{1}{2},n+1}-u_{\frac{1}{2},n-1})+\frac{b_{y_{\frac{1}{2},n}}}{4(h/2)^2}(u_{1,n+1}-u_{0,n+1}-u_{1,n-1}+u_{0,n-1})\\&+\frac{b_{x_{\frac{1}{2},n}}}{(h/2)^2}(u_{\frac{1}{2},n+1}+u_{\frac{1}{2},n-1}-2u_{\frac{1}{2},n})+\frac{b_{\frac{1}{2},n}}{2(h/2)^3}(u_{1,n+1}-u_{0,n+1}+u_{1,n-1}-u_{0,n-1}\\&-2(u_{1,n}-u_{0,n}))+\frac{(k^2u)_{1,n}-(k^2u)_{0,n}}{h}\Big]-a_{xx_{\frac{1}{2},n}}\frac{u_{1,n}-u_{0,n}}{h}-\frac{2a_{x_{\frac{1}{2},n}}}{a_{\frac{1}{2},n}}\Big(-(k^2u)_{\frac{1}{2},n}\\&-b_{y_{\frac{1}{2},n}}\frac{u_{\frac{1}{2},n+1}-u_{\frac{1}{2},n-1}}{h}-b_{\frac{1}{2},n}\frac{u_{\frac{1}{2},n+1}-2u_{\frac{1}{2},n}+u_{\frac{1}{2},n-1}}{(h/2)^2}-a_{x_{\frac{1}{2},n}}\frac{u_{1,n}-u_{0,n}}{h}\Big)+\mathcal{O}(h^2).\end{aligned}\tag{4.14}$$

Formulae (4.13) and (4.14) still contain the values of u at semi-integer grid locations. To have a scheme that would only operate with full-node values, we replace $u_{1/2,n}$ by the second order approximation

$$u_{\frac{1}{2},n}\approx\frac{u_{1,n}+u_{0,n}}{2},$$

and proceed similarly for the terms $u_{1/2,n+1}$, $u_{1/2,n-1}$, and $(k^2u)_{1/2,n}$. Using this modification, we obtain a fourth order accurate approximation of the boundary condition (4.9b) in the form:

$$\Big(\frac{u_{1,n}-u_{0,n}}{h}-\frac{h^2}{24}u_{xxx_{\frac{1}{2},n}}\Big)-ik\Big(\frac{u_{1,n}+u_{0,n}}{2}-\frac{h^2}{8}u_{xx_{\frac{1}{2},n}}\Big)=0,\tag{4.15}$$

where the terms $u_{xx_{1/2,n}}$ and $u_{xxx_{1/2,n}}$ are evaluated according to (4.13) and (4.14), respectively. Similarly, the boundary condition (4.9a) is approximated as

$$\Big(\frac{u_{M,n}-u_{M-1,n}}{h}-\frac{h^2}{24}u_{xxx_{M-\frac{1}{2},n}}\Big)+ik\Big(\frac{u_{M,n}+u_{M-1,n}}{2}-\frac{h^2}{8}u_{xx_{M-\frac{1}{2},n}}\Big)=0,\tag{4.16}$$

where the terms $(u_{xx})_{M-1/2,n}$ and $(u_{xxx})_{M-1/2,n}$ are evaluated according to the analogues of (4.13) and (4.14), respectively.

The results of computations with Sommerfeld-type boundary conditions are reported in Section 5.2. We emphasize that even though we set boundary conditions of different types on the adjacent sides of the rectangle [Sommerfeld and Dirichlet, see formulae (4.9a), (4.9b) and (4.10)], our numerical experiments show that this does not lead to any problems related to the corners of the domain.

5 Numerical results

To achieve the desired fourth order of accuracy in our compact finite difference approximation, the test solutions $u=u(x,y)$ for Eq. (4.1) must be at least 6 times continuously differentiable. Additionally, to satisfy the boundary condition (4.2) or boundary conditions (4.9), it is also convenient to choose the solution to be compactly supported inside the square D. We have found it easiest to devise such test solutions using polar coordinates, and then convert back to Cartesian coordinates for the actual computations. Specifically, we take a smooth and compactly supported function of r and multiply it by a smooth 2π periodic function of θ for generality. In doing so, to guarantee regularity at $r=0$, we additionally require that the function of r be equal to zero at the origin along with sufficiently many of its derivatives. Then, we substitute the resulting

$$u(r,\theta)=u\Big(\sqrt{x^2+y^2},\arctan\big(y/x\big)\Big)$$

into the left-hand side of Eq. (4.1) and derive the right-hand side $f=f(x,y)$, which is subsequently used in the scheme.

Our implementation was written in MATLAB, and the linear system obtained from our scheme is solved via MATLAB's built-in direct sparse solver. The computations were performed on a 2.16 GHz Intel Core 2 Duo MacBook Pro with 2 Gb of RAM running on Mac OS X.

The results in the following examples demonstrate fourth order convergence with respect to the grid size, and a somewhat faster than linear growth of the time required to compute the solution.

5.1 Dirichlet boundary condition

5.1.1 Example 1

For our first example, we use a test solution u, based on a trigonometric function of r, and coefficients a and b as follows:

$$\begin{aligned} u(x,y)&=\begin{cases}\sin^6(2r)\cos(\theta), & r<\frac{\pi}{2},\\ 0, & r>\frac{\pi}{2},\end{cases}\\ &=\begin{cases}\sin^6(2\sqrt{x^2+y^2})\cos(\arctan(y/x)), & r<\frac{\pi}{2},\\ 0, & r>\frac{\pi}{2},\end{cases}\end{aligned}$$

$$a(x,y)=1+e^{-x^2-y^2},$$
$$b(x,y)=1+\frac{x^2+y^2}{1+x^2+y^2}.$$

The domain in this case is a square of side length $s=4$, centered at the origin. The value of k was chosen to be $k=1$. Note, that in this case

$$\nu=\min_{(x,y)\in D}\{a(x,y),b(x,y)\}=\min\{1+e^{-2\pi^2},1+0\}=1,$$

and so we see that (4.8) is satisfied since

$$\frac{2\pi^2\nu}{s^2}=\frac{2\pi^2}{16}\approx 1.2337>1=k^2.$$

Table 1 compares the error of the numerical and exact solutions on a series of grids of step-sizes h given in the leftmost column. From column 3 we clearly see the fourth order convergence. Column 5 shows that computational complexity of the direct solver scales somewhat faster than linear as the grid is refined.

Table 1: Grid convergence and matrix inversion times for Example 1, $k=1$.

h	$\|\|u-u_{num}\|\|_\infty$	Convergence Rate	Time(s)	Time Scaling
1/4	1.6539×10^{-2}	-	4.6021×10^{-3}	-
1/8	1.1852×10^{-3}	3.7355	2.1428×10^{-2}	4.6562
1/16	8.2482×10^{-5}	3.7907	.10537	4.9174
1/32	5.2872×10^{-6}	3.9497	.5424	5.1475
1/64	3.3186×10^{-7}	3.9915	3.4023	6.2726
1/128	2.0752×10^{-8}	3.9990	22.800	6.7014

5.1.2 Example 2

In this example, we use a test solution u which is derived from a polynomial in r, with a and b as follows:

$$u(x,y)=\begin{cases} r^6(1-r^2)^6\sin(\theta), & r<1,\\ 0, & r>1,\end{cases}$$
$$=\begin{cases} (x^2+y^2)^3(1-x^2-y^2)^6\sin(\arctan(y/x)), & r<1,\\ 0, & r>1,\end{cases}$$
$$a(x,y)=1+\frac{\arctan(xy)}{2\pi},$$
$$b(x,y)=1+\frac{x^2+y^2}{1+x^2+y^2}.$$

Note, that a is an asymmetric function of x and y, whereas both a and b were radially symmetric in the first example. The domain is a square of side length $s=4$ centered at the origin. We choose $k=1$ and so (4.8) is satisfied since

$$\nu=\min_{(x,y)\in\bar{D}}\{a(x,y),b(x,y)\}=\min\left\{1+\frac{\arctan(-1)}{2\pi},1+0\right\}=\frac{7}{8},$$

and

$$\frac{2\pi^2\nu}{s^2}=\frac{2\pi^2(7/8)}{16}\approx 1.0795>1=k^2.$$

The computational results are summarized in Table 2. Column 3 clearly shows the fourth order convergence.

Table 2: Grid convergence and matrix inversion times for Example 2, $k=1$.

h	$\|\|u-u_{num}\|\|_\infty$	Convergence Rate	Time(s)	Time Scaling
1/4	2.1504×10^{-3}	-	4.9804×10^{-3}	-
1/8	6.1167×10^{-5}	5.9293	1.7237×10^{-2}	3.4610
1/16	2.0265×10^{-6}	5.4940	9.3481×10^{-2}	5.4232
1/32	1.2938×10^{-7}	3.9577	.50478	5.3999
1/64	7.6192×10^{-9}	4.1207	3.4859	6.9057
1/128	4.6582×10^{-10}	4.0443	13.129	3.7662

5.1.3 Example 3

We now use a test solution u which includes an exponential function in r:

$$u(x,y)=\begin{cases}(1-r^2)^6(1-e^{-r^2})^6\sin(\cos(\theta)), & r<1,\\ 0, & r>1,\end{cases}$$
$$=\begin{cases}(1-x^2-y^2)^6(1-e^{-x^2-y^2})^6\sin(\cos(\arctan(y/x))), & r<1,\\ 0, & r>1,\end{cases}$$
$$a(x,y)=1+\frac{\arctan(x+y)}{2\pi},$$
$$b(x,y)=1+\frac{e^{-x^2-y^2}}{1+e^{-x^2-y^2}}.$$

The domain is a square of side length $s=4$ centered at the origin. We choose $k=1$ and verify that (4.8) is satisfied. We have

$$\nu=\min_{(x,y)\in\bar{D}}\{a(x,y),b(x,y)\}=\min\left\{1+\frac{\arctan(-2)}{2\pi},1\right\}\approx 0.8238,$$

and

$$\frac{2\pi^2\nu}{s^2}\approx\frac{2\pi^2(0.8238)}{16}\approx 1.0163>1=k^2.$$

Table 3: Grid convergence and matrix inversion times for Example 3, $k=1$.

h	$\|\|u-u_{num}\|\|_\infty$	Convergence Rate	Time(s)	Time Scaling
1/4	7.2679×10^{-5}	-	4.0316×10^{-3}	-
1/8	3.0646×10^{-6}	4.8698	1.7305×10^{-2}	4.2924
1/16	9.0079×10^{-8}	5.8328	9.7753×10^{-2}	5.6489
1/32	5.7535×10^{-9}	3.9568	.61776	6.3196
1/64	3.3678×10^{-10}	4.1333	3.3931	5.4926
1/128	2.0400×10^{-11}	4.0631	22.082	6.5078

Table 3 summarizes the numerical results. As before, column 3 demonstrates the fourth order convergence, and column 5 shows that computational complexity scales faster than linear as the grid dimension increases.

5.2 Sommerfeld-type boundary conditions

We re-run the three examples of Section 5.1, but for higher values of the wavenumber, $k=20$ and $k=40$. To avoid resonances, i.e., guarantee uniqueness of the solution, we use a Sommerfeld-type boundary condition (4.9), approximated with fourth order accuracy as in (4.15) instead of the Dirichlet boundary condition (4.2). In all of the following computations, we take a square domain of side length $s=4$. Other than the change in the boundary conditions and the value of k, Examples 4, 5, and 6 and Examples 7, 8, and 9 use the exact same test solutions and coefficients of the Helmholtz equation as Examples

Example 4

Table 4: Grid convergence and matrix inversion times for Example 4, $k=20$.

h	$\|\|u-u_{num}\|\|_\infty$	Convergence Rate	Time(s)	Time Scaling
1/8	2.0126×10^{-3}	-	3.4113×10^{-2}	-
1/16	1.0670×10^{-4}	4.3432	0.19399	5.6868
1/32	6.3499×10^{-6}	4.0991	1.0658	5.5080
1/64	4.0061×10^{-7}	3.9813	7.2026	6.7409
1/128	2.5054×10^{-8}	3.9987	48.745	6.7677

Example 5

Table 5: Grid convergence and matrix inversion times for Example 5, $k=20$.

h	$\|\|u-u_{num}\|\|_\infty$	Convergence Rate	Time(s)	Time Scaling
1/8	4.6930×10^{-4}	-	2.9426×10^{-2}	-
1/16	1.5384×10^{5}	5.5232	.20017	6.8024
1/32	8.9785×10^{-7}	4.1393	1.1548	5.7688
1/64	4.8405×10^{-8}	4.3068	8.3947	7.2697
1/128	2.7099×10^{-9}	4.2263	53.000	6.3135

1, 2, and 3, respectively, presented in Section 5.1. We note that as all our test solutions are compactly supported inside the square computational domain, they satisfy the boundary conditions (4.9). The third column of Tables 4, 5, and 6 and Tables 7, 8, and 9 clearly demonstrates the fourth order convergence in each of the examples.

Example 6

Table 6: Grid convergence and matrix inversion times for Example 6, $k=20$.

h	$\|\|u-u_{num}\|\|_\infty$	Convergence Rate	Time(s)	Time Scaling
1/8	1.6277×10^{-5}	-	3.4923×10^{-2}	-
1/16	3.7661×10^{-7}	6.5743	.21660	6.2024
1/32	2.3499×10^{-8}	4.0033	1.2078	5.5760
1/64	1.4508×10^{-9}	4.0246	7.4962	6.2065
1/128	8.9214×10^{-11}	4.0327	59.104	7.8845

Example 7

Table 7: Grid convergence and matrix inversion times for Example 7, $k=40$.

h	$\|\|u-u_{num}\|\|_\infty$	Convergence Rate	Time(s)	Time Scaling
1/8	1.3362×10^{-4}	-	1.7520×10^{-2}	-
1/16	1.7489×10^{-5}	2.7640	.15897	9.0737
1/32	9.3741×10^{-7}	4.3194	1.0825	6.8094
1/64	5.3381×10^{-8}	4.1905	8.1212	7.5021
1/128	3.4192×10^{-9}	3.9512	57.942	7.1347

Example 8

Table 8: Grid convergence and matrix inversion times for Example 8, $k=40$.

h	$\|\|u-u_{num}\|\|_\infty$	Convergence Rate	Time(s)	Time Scaling
1/8	1.2893×10^{-5}	-	3.3510×10^{-2}	-
1/16	7.2638×10^{-6}	1.3323	.18749	5.5950
1/32	2.7735×10^{-7}	5.1176	1.1141	5.9422
1/64	3.9907×10^{-8}	2.6363	10.869	9.7563
1/128	2.1505×10^{-9}	4.3077	46.765	4.3025

Example 9

Table 9: Grid convergence and matrix inversion times for Example 9, $k=40$.

h	$\|\|u-u_{num}\|\|_\infty$	Convergence Rate	Time(s)	Time Scaling
1/8	5.1486×10^{-7}	-	3.3502×10^{-2}	-
1/16	2.9599×10^{-7}	1.3189	.18520	5.5281
1/32	1.1909×10^{-8}	4.9855	1.5352	8.2894
1/64	7.4657×10^{-10}	3.9939	7.6294	4.9696
1/128	4.7180×10^{-11}	3.9779	41.294	5.4124

5.3 Comparison to the second order scheme

To demonstrate the gains provided by the proposed fourth order method, we recompute the solutions that correspond to $k=40$ using the standard central difference second order scheme written on a five node stencil. All the settings and parameters for Examples 10, 11, and 12 below are exactly the same as those for Examples 7, 8, and 9 in Section 5.2, except for the change in the discretization. The results of second order computations are summarized in Tables 10, 11, and 12. The third column of each table corroborates the anticipated rate of grid convergence.

Example 10

Table 10: Grid convergence and matrix inversion times for Example 10.

h	$\|\|u-u_{num}\|\|_\infty$	Convergence Rate	Time(s)	Time Scaling
1/8	1.7131×10^{-3}	-	2.1341×10^{-2}	-
1/16	5.0216×10^{-4}	1.8470	.11583	5.4274
1/32	1.4332×10^{-4}	1.8718	.67270	5.8079
1/64	3.0600×10^{-5}	2.1641	3.8144	5.6703
1/128	7.6862×10^{-6}	1.9953	25.660	6.7269

Example 11

Table 11: Grid convergence and matrix inversion times for Example 11.

h	$\|\|u-u_{num}\|\|_\infty$	Convergence Rate	Time(s)	Time Scaling
1/8	3.2175×10^{-5}	-	1.6759×10^{-2}	-
1/16	4.7681×10^{-5}	.82146	.10944	6.5301
1/32	1.4624×10^{-5}	1.8057	.64743	5.9158
1/64	2.9564×10^{-6}	2.2241	3.9461	6.0951
1/128	4.2946×10^{-7}	2.6237	25.098	6.3602

Example 12

Table 12: Grid convergence and matrix inversion times for Example 12.

h	$\|\|u-u_{num}\|\|_\infty$	Convergence Rate	Time(s)	Time Scaling
1/8	9.7856×10^{-7}	-	1.9636×10^{-2}	-
1/16	5.0916×10^{-7}	1.3863	.12473	6.3524
1/32	2.5638×10^{-7}	1.4092	.67060	5.3763
1/64	5.8207×10^{-8}	2.0987	3.8213	5.6983
1/128	1.5103×10^{-8}	2.9631	25.046	6.5543

To compare the performance of the new compact fourth order scheme against that of the standard second order scheme, we plot the error versus the grid size and the matrix inversion time versus the grid size for both schemes on the same figure. Figs. 1 and 2

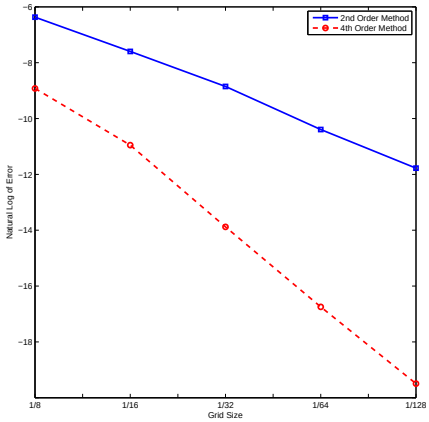

Figure 1: Logarithmic plot of error versus grid size for the 2nd and 4th order methods applied to Examples 7 and 10.

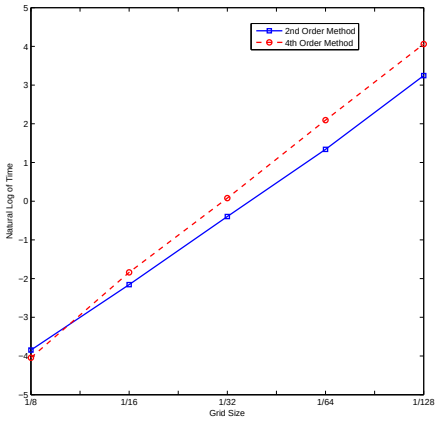

Figure 2: Logarithmic plot of time versus grid size for the 2nd and 4th order methods applied to Examples 7 and 10. Difference at $h=1/128$ is 32.282 seconds.

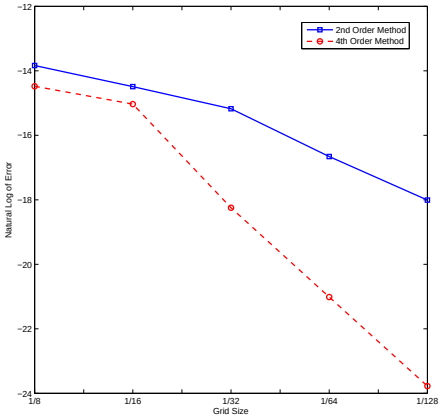

Figure 3: Logarithmic plot of error versus grid size for the 2nd and 4th order methods applied to Examples 8 and 11.

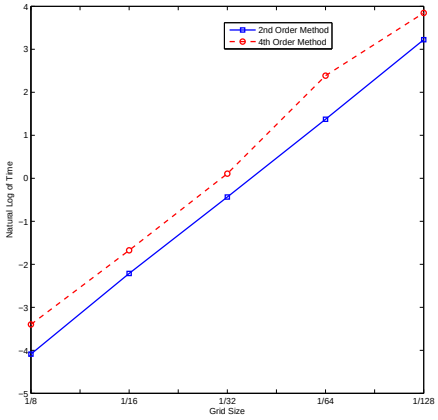

Figure 4: Logarithmic plot of time versus grid size for the 2nd and 4th order methods applied to Examples 8 and 11. Difference at $h=1/128$ is 21.667 seconds.

below correspond to Examples 7 and 10, Figs. 3 and 4 correspond to Examples 8 and 11, and Figs. 5 and 6 correspond to Examples 9 and 12. We see that for roughly twice the computational effort or less on every given grid, the fourth order method enables a major improvement in accuracy. Fig. 1 shows, for example, that the accuracy attained by the second order scheme on the grid with size $h=1/128$ is achieved by the fourth order scheme already between $h=1/16$ and $h=1/32$. Hence, for a fixed accuracy the fourth order method requires about 20 to 25 per cent less CPU time to solve the linear system in addition to a reduced storage by a factor of about 4 in each direction.

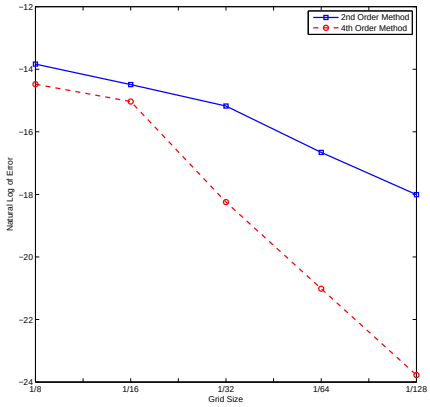

Figure 5: Logarithmic plot of error versus grid size for the 2nd and 4th order methods applied to Examples 9 and 12.

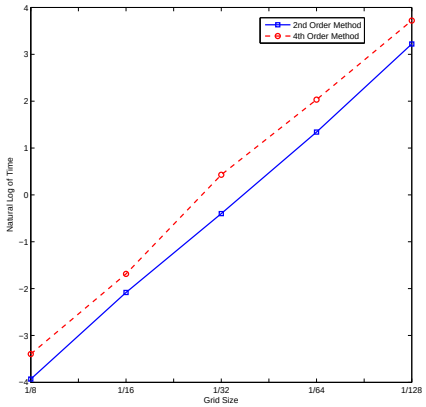

Figure 6: Logarithmic plot of time versus grid size for the 2nd and 4th order methods applied to Examples 9 and 12. Difference at $h=1/128$ is 16.248 seconds.

Moreover, to better understand the overall computational cost, we have analyzed separately its other major component–the cost of setting up the matrix. For Examples 9 and 12 on the grid with size $h=1/128$, the time to set up the matrix was 31.078 seconds for the new compact fourth order method based on a 9-point stencil, and 12.229 seconds for the central difference second order method based on a 5-point stencil. This is not surprising given that the matrix of the 9-point scheme will have approximately twice as many non-zero entries compared to the matrix of the 5-point scheme, and also that individual coefficients of the fourth order scheme are given by more elaborate expressions. We expect though that as the mesh gets finer or we treat three dimensional problems, the setup time will become insignificant relative to the solution time. This is also true if multiple problems are solved with different boundary conditions or right hand sides where changes to the matrix are minimal.

6 Discussion

We have developed and tested a fourth order accurate finite difference scheme for the variable coefficient Helmholtz equation. In doing so, the variation of coefficients is allowed under the first derivatives in the second order differential operator. Elliptic PDEs of this type appear in many applications, for example, the propagation of time-harmonic electromagnetic waves through the media with variable permittivity, or the propagation of time-harmonic acoustic waves through the media with variable speed of sound.

In two space dimensions, the proposed scheme uses a compact 3×3 stencil. The design fourth order convergence rate of the scheme has been corroborated experimentally for a variety of cases, including those with a high wavenumber k.

A fourth order scheme has a reduced phase error compared with a second order

scheme [15], and so reduces the pollution error. Direct numerical comparison of the new fourth order scheme with the standard central difference second order scheme shows substantial gains in accuracy.

A key advantage of the proposed scheme is that its narrow 3×3 stencil yields a second order finite difference equation (whereas the order of accuracy is fourth). As the order of the difference equation matches that of the original differential equation, the scheme requires no additional boundary conditions beyond those needed for the differential equation itself. In contradistinction to that, a fourth order accurate scheme on the conventional broad stencil yields a fourth order difference equation and so requires an extra pair of boundary conditions, see, e.g., [4, 12, 13].

Another advantage of the proposed scheme is that the resultant matrix has a narrower bandwidth. Indeed, for an $N\times N$ Cartesian grid the dimension of the matrix is $N^2\times N^2$, and the bandwidth is $\sim 2(N+1)+1$. This is close to the bandwidth that characterizes the central difference second order scheme, $\sim 2N+1$; and experimentally, we have seen that the cost of inverting the matrix by a direct method in the fourth order case does not exceed that for the second order case by more than roughly a factor of two. If, however, the conventional broad stencil is used to build a fourth order approximation, then the bandwidth of the matrix becomes $\sim 4N+1$. Hence, one can expect that direct solvers will perform better for the compact scheme than for the conventional fourth order scheme. Moreover, we are not aware of any efficient reordering strategies in the literature that would help reduce the bandwidth from about $4N$ to somewhere around $2N$. This is especially true as reordering is thought to be most useful when applied to real positive definite matrices [9, 10, 14], whereas our matrices are never positive definite, often not symmetric either, and may even have complex entries (in the case of Sommerfeld-type boundary conditions). On the other hand, in the future we plan to transition from direct solvers to iterative solvers. In that case, the bandwidth will become less of an issue. However, the ease of setting the boundary conditions will still remain attractive.

We emphasize that our scheme is expected to attain its design accuracy only for sufficiently smooth coefficients. It is not our intention to use the proposed scheme directly for solving differential equations with discontinuous coefficients. Indeed, discontinuities in $a(x,y)$ or $b(x,y)$ will lead to the loss of accuracy (of this scheme, as well as of any other scheme, if implemented in a direct way) and hence to a deterioration of performance. To analyze the propagation of waves through the more realistic inhomogeneous media that involve material discontinuities, we will combine the proposed scheme with the methodology based on Calderon's projections and the method of difference potentials, see [21, 27]. This methodology does not involve any one-sided differencing or other features that may adversely affect its numerical performance and/or lead to non-physical effects. Yet it allows to accommodate complex geometries on regular structured grids with no loss of accuracy. In doing so, the variation of coefficients presents no obstacle, unlike methods based on boundary integral equations.

The proposed fourth order accurate scheme has been extended to three space dimensions where it uses a compact $3\times3\times3$ stencil.

Acknowledgments

This work was partially supported by the United States–Israel Binational Science Foundation (BSF), grant number 2008094. Research of the first and second authors was also supported in part by the US Air Force, grant number FA9550-07-1-0170, and US NSF, grant number DMS-0810963.

References

[1] M. S. Agranovich, Spectral properties of diffraction problems, In N. N. Voitovich, B. Z. Katsenelenbaum and A. N. Sivov, editors, Method of Generalized Resonances in Diffraction Theory, Nauka, Moscow, 1977, [in Russian].

[2] M. S. Agranovich, B. Z. Katsenelenbaum, A. N. Sivov and N. N. Voitovich, Generalized Method of Eigenoscillations in Diffraction Theory, WILEY-VCH Verlag Berlin GmbH, Berlin, 1999, Translated from the Russian Manuscript by Vladimir Nazaikinskii.

[3] Ivo M. Babuška and Stefan A. Sauter, Is the pollution effect of the FEM avoidable for the Helmholtz equation considering high wave numbers?, SIAM Rev., 42(3) (2000), 451–484 (electronic), reprint of SIAM J. Numer. Anal., 34(6) (1997), 2392–2423, [MR1480387 (99b:65135)].

[4] G. Baruch, G. Fibich and S. Tsynkov, High-order numerical method for the nonlinear Helmholtz equation with material discontinuities in one space dimension, J. Comput. Phys., 227 (2007), 820–850.

[5] G. Baruch, G. Fibich and S. Tsynkov, A high-order numerical method for the nonlinear Helmholtz equation in multidimensional layered media, J. Comput. Phys., 228 (2009), 3789–3815.

[6] A. Bayliss, C. I. Goldstein and E. Turkel, On accuracy conditions for the numerical computation of waves, J. Comput. Phys., 59(3) (1985), 396–404.

[7] D. Steven Britt, Semyon Tsynkov and Eli Turkel, A compact fourth order scheme for the Helmholtz equation in polar coordinates, J. Sci. Comput., 2010, accepted for publication.

[8] J. E. Caruthers, J. S. Steinhoff and R. C. Engels, An optimal finite difference representation for a class of linear PDE's with application to the Helmholtz equation, J. Comput. Acoust., 7(4) (1999), 245–252.

[9] Timothy A. Davis, Direct methods for sparse linear systems, Volume 2 of Fundamentals of Algorithms, Society for Industrial and Applied Mathematics (SIAM), Philadelphia, PA, 2006.

[10] Iain S. Duff and Stéphane Pralet, Strategies for scaling and pivoting for sparse symmetric indefinite problems, SIAM J. Matrix. Anal. Appl., 27(2) (2005), 313–340 (electronic).

[11] Y. Erlangga and E. Turkel, Iterative schemes for high order compact discretizations to the exterior Helmholtz equation, M2AN, 2009, submitted for publication.

[12] G. Fibich and S. V. Tsynkov, High-order two-way artificial boundary conditions for nonlinear wave propagation with backscattering, J. Comput. Phys., 171 (2001), 632–677.

[13] G. Fibich and S. V. Tsynkov, Numerical solution of the nonlinear Helmholtz equation using nonorthogonal expansions, J. Comput. Phys., 210(1) (2005), 183–224.

[14] M. Hagemann and O. Schenk, Weighted matchings for preconditioning symmetric indefinite linear systems, SIAM J. Sci. Comput., 28(2) (2006), 403–420 (electronic).

[15] I. Harari and E. Turkel, Accurate finite difference methods for time-harmonic wave propagation, J. Comput. Phys., 119(2) (1995), 252–270.
[16] Heinz-Otto Kreiss and N. Anders Petersson, A second order accurate embedded boundary method for the wave equation with Dirichlet data, SIAM J. Sci. Comput., 27(4) (2006), 1141–1167 (electronic).
[17] Heinz-Otto Kreiss, N. Anders Petersson and Jacob Yström, Difference approximations for the second order wave equation, SIAM J. Numer. Anal., 40(5) (2002), 1940–1967 (electronic).
[18] M. Nabavi, K. Siddiqui and J. Dargahi, A new 9-point sixth-order accurate compact finite-difference method for the Helmholtz equation, J. Sound. Vibrat., 307 (2007), 972–982.
[19] J. W. Nehrbass, J. O. Jevtic and R. Lee, Reducing the phase error for finite-difference methods without incresing the order, IEEE Trans. Antenna. Propagat., 46 (1998), 1194–1201.
[20] Stefan Nilsson, N. Anders Petersson, Björn Sjögreen and Heinz-Otto Kreiss, Stable difference approximations for the elastic wave equation in second order formulation, SIAM J. Numer. Anal., 45(5) (2007), 1902–1936.
[21] V. S. Ryaben'kii, Method of Difference Potentials and Its Applications, Volume 30 of Springer Series in Computational Mathematics, Springer-Verlag, Berlin, 2002.
[22] I. Singer and E. Turkel, High-order finite difference methods for the Helmholtz equation, Comput. Methods. Appl. Mech. Engrg., 163(1-4) (1998), 343–358.
[23] I. Singer and E. Turkel, Sixth-order accurate finite difference schemes for the Helmholtz equation, J. Comput. Acoust., 14(3) (2006), 339–351.
[24] V. I. Smirnov, Course of Higher Mathematics, Vol. IV, Part 1, Nauka, Moscow, Sixth revised edition, 1974, [in Russian].
[25] V. I. Smirnov, Course of Higher Mathematics, Vol. IV, Part 2, Nauka, Moscow, Sixth revised edition, 1981, [in Russian].
[26] G. Sutmann, Compact finite difference schemes of sixth order for the Helmholtz equation, J. Comput. Appl. Math., 203(1) (2007), 15–31.
[27] S. V. Tsynkov, On the definition of surface potentials for finite-difference operators, J. Sci. Comput., 18(2) (2003), 155–189.